Published in final edited form as:

Eur J Nucl Med Mol Imaging. 2021 July ; 48(7): 2259–2271. doi:10.1007/s00259-020-05152-8.

Comparing ATN-T designation by tau PET visual reads, tau PET quantification, and CSF PTau181 across three cohorts

Karine Provost[1], **Leonardo Iaccarino**[1], **David N. Soleimani-Meigooni**[1,2], **Suzanne Baker**[2], **Lauren Edwards**[1], **Udo Eichenlaub**[3], **Oskar Hansson**[4], **William Jagust**[2,5], **Mustafa Janabi**[2], **Renaud La Joie**[1], **Orit Lesman-Segev**[1], **Taylor J. Mellinger**[1], **Bruce L. Miller**[1], **Rik Ossenkoppele**[4,6], **Julie Pham**[1], **Ruben Smith**[4], **Ida Sonni**[2,7], **Amelia Strom**[1], **Niklas Mattsson-Carlgren**[4,8,9], **Gil D. Rabinovici**[1,2,5,10] **Alzheimer's Disease Neuroimaging Initiative (ADNI)**

[1]Memory and Aging Center, Department of Neurology, University of California San Francisco, 675 Nelson Rising Lane, Suite 190, San Francisco, CA 94143, USA [2]Lawrence Berkeley National Laboratory, Berkeley, CA, USA [3]Roche Diagnostics GmbH, Penzberg, Germany [4]Clinical Memory Research Unit, Lund University, Lund, Sweden [5]Helen Wills Neuroscience Institute, UC Berkeley, Berkeley, CA, USA [6]Alzheimer Center Amsterdam, Department of Neurology, Amsterdam Neuroscience, Vrije Universiteit Amsterdam, Amsterdam UMC, Amsterdam, the Netherlands [7]Ahmanson Translational Theranostics Division, Department of Molecular and Medical Pharmacology, UC Los Angeles, Los Angeles, CA, USA [8]Department of Neurology, Skåne University Hospital, Lund, Sweden [9]Wallenberg Centre for Molecular Medicine, Lund University, Lund, Sweden [10]Department of Radiology and Biomedical Imaging, University of California San Francisco, San Francisco, CA, USA

Abstract

Karine Provost, provost.karine@gmail.com.

Data used in preparation of this article were obtained from the Alzheimer's Disease Neuroimaging Initiative (ADNI) database (adni.loni.usc.edu). As such, the investigators within the ADNI contributed to the design and implementation of ADNI and/or provided data but did not participate in analysis or writing of this report. A complete listing of ADNI investigators can be found at http://adni.loni.usc.edu/wp-content/uploads/how_to_apply/ADNI_Acknowledgement_List.pdf

Supplementary Information The online version contains supplementary material available at https://doi.org/10.1007/s00259-020-05152-8.

Conflict of interest U.E. is an employee of Roche. O.H. has received research support (for the institution) from Roche, GE Healthcare, Biogen, AVID Radiopharmaceuticals, Fujirebio, and Euroimmun. In the past 2 years, he has received consultancy/speaker fees (paid to the institution) from Lilly, Roche, and Fujirebio. B.L.M. serves as Medical Director for the John Douglas French Foundation; Scientific Director for the Tau Consortium; Director/Medical Advisory Board of the Larry L. Hillblom Foundation; Scientific Advisory Board Member for the National Institute for Health Research Cambridge Biomedical Research Centre and its subunit, the Biomedical Research Unit in Dementia (UK); and Board Member for the American Brain Foundation. W.J. has served as a consultant to Genentech, Biogen, Bioclinica, CuraSen, and Grifols. G.D.R. receives research support from Avid Radiopharmaceuticals, GE Healthcare, and Life Molecular Imaging and has received consulting fees or speaking honoraria from Axon Neurosciences, Roche, Eisai, and Genentech. All other authors have no relevant financial or non-financial interests to disclose.

Ethics approval This study was performed in line with the principles of the Declaration of Helsinki. The study was approved by the University of California (San Francisco and Berkeley), Lawrence Berkeley National Laboratory (LBNL), and the Ethical Committee of Lund University, Sweden, institutional review boards for human research. Each ADNI study site received approval from its institutional ethical standards committee on human experimentation.

Consent to participate/publish Written informed consent was obtained from all participants or their surrogates.

Purpose—To compare rates of tau biomarker positivity (T-status) per the 2018 Alzheimer's Disease (AD) Research Framework derived from [^{18}F]flortaucipir (FTP) PET visual assessment, FTP quantification, and cerebrospinal fluid (CSF) phosphorylated Tau-181 (PTau181).

Methods—We included 351 subjects with varying clinical diagnoses from three cohorts with available FTP PET and CSF PTau181 within 18 months. T-status was derived from (1) FTP visual assessment by two blinded raters; (2) FTP standardized uptake value ratio (SUVR) quantification from a temporal meta-ROI (threshold: SUVR ≥1.27); and (3) Elecsys® Phospho-Tau (181P) CSF (Roche Diagnostics) concentrations (threshold: PTau181 ≥ 24.5 pg/mL).

Results—FTP visual reads yielded the highest rates of T+, while T+ by SUVR increased progressively from cognitively normal (CN) through mild cognitive impairment (MCI) and AD dementia. T+ designation by CSF PTau181 was intermediate between FTP visual reads and SUVR values in CN, similar to SUVR in MCI, and lower in AD dementia. Concordance in T-status between modality pairs ranged from 68 to 76% and varied by clinical diagnosis, being highest in patients with AD dementia. In discriminating Aβ + MCI and AD subjects from healthy controls and non-AD participants, FTP visual assessment was most sensitive (0.96) but least specific (0.60). Specificity was highest with FTP SUVR (0.91) with sensitivity of 0.89. Sensitivity (0.73) and specificity (0.72) were balanced for PTau181.

Conclusion—The choice of tau biomarker may differ by disease stage and research goals that seek to maximize sensitivity or specificity. Visual interpretations of tau PET enhance sensitivity compared to quantification alone, particularly in early disease stages.

Keywords

Tau; PET; Flortaucipir; Alzheimer's disease; Biomarkers; CSF

Introduction

Alzheimer's disease (AD) clinical research has been transformed by the advent of in vivo biomarkers for amyloid-beta (Aβ) and tau, the proteins that form the plaques and tangles that define AD neuropathology [1–4]. Correct identification of biomarker status is important for screening participants and for outcome evaluation in clinical trials of novel diseasemodifying therapies [5, 6]. The AT(N) research framework [7] proposes binary classification of all individuals as positive or negative for amyloid, tau, and neurodegeneration, allowing interchangeable use of cerebrospinal fluid (CSF) or imaging measures. While previous work has compared neuroimaging and CSF classification of amyloid and neurodegeneration, few studies have compared fluid and imaging definitions of T-status [8–16].

Tau positron emission tomography (PET) is frequently analyzed using semi-quantitative metrics such as the standardized uptake value ratio (SUVR), commonly considering a region of interest (ROI) consisting of brain regions involved early in disease course, such as a temporal lobe region of interest (meta-ROI) [17–19]. Independent studies have indicated different meta-ROI SUVR thresholds for positivity, typically ranging between SUVR 1.2 and 1.4 [8, 17–20]. The accuracy of semi-quantitative metrics, however, can be affected by multiple determinants, including partial volume, threshold effects, and spillover from off-

target areas [1, 21]. Quantification of tau PET data also requires access to structural magnetic resonance imaging (MRI) and adequate co-registration.

In contrast to SUVR quantification, visual interpretation of tau PET allows for assessment of topography of binding and may lead to detection of significant focal signal. However, a widely accepted standard for interpretation is currently lacking. A visual rating algorithm has been recently proposed by Fleisher et al., with high accuracy for detection of Braak stage V–VI neurofibrillary tangles and high Alzheimer's disease neuropathological changes (ADNC) at autopsy using [^{18}F]flortaucipir (FTP) [22]. Visual interpretation of FTP PET is likely to gain importance given the recent Food and Drug Administration approval of this tracer for clinical use in the USA.

CSF-based analyses of phospho-Tau (PTau181) have been well validated and are commonly used [23]. However, it has been proposed that analytical methodology, including type of assay, can considerably influence measures of PTau181 concentrations [6, 24, 25]. The Elecsys® Phospho-Tau (181P) CSF assay (Roche Diagnostics International Ltd., Rotkreuz, Switzerland) is a fully automated electrochemiluminescence immunoassay with increased reproducibility across multiple sites compared to other available assays [25, 26]. The literature on comparative analysis of this assay with tau PET is limited [8, 27].

In contrast to amyloid biomarkers for which CSF and PET show high concordance [28–31], agreement between PET and CSF-based biomarkers of tau pathology is highly variable, ranging from 50 to 87%, and shows only modest correlation (r = 0.29 to 0.75) [8–16, 27, 32–34], largely impacted by methodology and technical factors. The objectives of this study were to perform cross-validation of different biomarkers of tau in a cohort of patients with neurodegenerative conditions. In particular, we aimed to firstly assess concordance of binary T-status obtained by FTP visual assessment, SUVR quantification, and CSF PTau181; and secondly to compare sensitivity and specificity of each modality for distinguishing amyloid-positive patients with mild cognitive impairment (MCI) and dementia due to AD from other clinical groups.

Methods

Study population

The cohort consisted of a convenience sample of 351 participants enrolled in research studies at the University of California San Francisco Alzheimer's Disease Research Center (UCSF ADRC, n = 98), the Alzheimer's Disease Neuroimaging Initiative (ADNI, n = 179), and the Swedish BioFINDER study (n = 74). The participants spanned a wide range of clinical diagnoses (Supplementary Table 1), had undergone FTP PET between June 2014 and May 2019, had structural MRI available, and had undergone lumbar puncture within 18 months from the PET scan with available PTau181 Elecsys measurements (Supplementary Fig. 1).

Clinical diagnoses were made blinded to biomarker results, based on established criteria; participants were either cognitively unimpaired or assigned a diagnosis of MCI [35], probable AD dementia [36] (herein referred to as AD clinical diagnosis: AD_c), or non-AD

disorders (behavioral variant frontotemporal dementia [37], semantic or non-fluent variant primary progressive aphasia [38], corticobasal syndrome [39], progressive supranuclear palsy [40, 41], dementia with Lewy bodies [42], or vascular dementia [43]). Amyloid status was determined by PET or CSF (details can be found in Supplementary Table 2).

Some data used in the preparation of this article were obtained from the ADNI database (adni.loni.usc.edu). ADNI was launched in 2003 as a public-private partnership, led by Principal Investigator Michael W. Weiner, MD. The primary goal of ADNI has been to test whether serial MRI, PET, other biological markers, and clinical and neuropsychological assessment can be combined to measure the progression of MCI and early AD.

Written informed consent was obtained from all participants or their surrogates. The study was approved by local institutional review boards for human research.

FTP PET acquisition and processing

FTP PET acquisition and processing has been described in detail elsewhere [18, 19] (Supplementary Table 2). In brief, participants underwent FTP brain PET following injection of ~370 MBq at 80–100 min post-injection (UCSF and BioFINDER) or 75–105 min post-injection (ADNI). PET data was reconstructed using an iterative method with attenuation correction. Subjects also underwent MRI, which was used for PET processing only. FTP PET regional SUVR data was extracted in native space after co-registration to T1-weighted MRI with SPM12 and cortical parcellation with FreeSurfer (version 5.3, https://surfer.nmr.mgh.harvard.edu/). Reference region for FTP-PET was the inferior cerebellar gray matter [44]. Non-partial volume corrected data were used.

CSF analysis

CSF samples were collected following lumbar puncture and processed using established protocols (Supplementary Table 2). Samples were stored in polypropylene tubes at −60 °C or below until biomarker analysis. All samples were analyzed with the fully automated electrochemiluminescence immunoassay Elecsys Phospho-Tau (181P) CSF on a COBAS E 601 analyzer (Roche Diagnostics International Ltd., Rotkreuz, Switzerland). Samples from UCSF and BioFINDER cohorts were analyzed at the Clinical Neurochemistry Laboratory, University of Gothenburg, Sweden, and samples from ADNI were analyzed at the University of Pennsylvania biomarker core laboratory [25, 45].

T-status definition

T-status based on visual assessment of FTP PET scans—Anonymized images were independently assessed by two raters (one nuclear medicine physician, K.P. and one behavioral neurologist, D.S.M., both with experience in interpreting brain PET scans). Raters were blinded to all clinical information, amyloid status, CSF results, and SUVR quantification values. In addition, intensity-normalized SUVR images were multiplied by a random factor to ensure blinding to SUVR values during interpretation. Images were viewed on MRIcron (https://www.nitrc.org/projects/mricron) using the NIH color scale. Raters manually thresholded images to adjust contrast so that inferior cerebellar gray matter appeared as pale green to light blue (roughly equivalent to an upper threshold of 2.2–2.5

SUVR). A total of 47 scans (randomly sampled) were duplicated and were read twice by each rater to assess intra-rater reliability.

Visual assessment was based on a priori criteria (Fig. 1), previously described [46]. Images were assigned T+ status if there was an AD-like pattern of binding (i.e., moderate-to-intense signal in the parieto-temporal cortex, following typical Braak and Braak distribution) [47, 48] or if there was significant, confluent binding restricted to the temporal lobes. A T-status was assigned if the FTP was within normal limits (including within the expected range of off-target binding for this tracer [1, 21]) or was suggestive of a non-AD pattern of binding (for example, extensive binding in the frontal white matter). This visual interpretation scheme is similar although not identical to the approach described by Fleisher et al. that received FDA regulatory approval [22].

In case of discordance in T-status between the two raters, consensus was obtained from a third independent rater (radiologist O.L.S. or neurologist R.S. with experience in interpreting FTP PET), blinded to all clinical information and to the interpretation of the other two raters. In such cases, the majority (two out of three) T-status was used.

T-status based on FTP SUVR quantification—A bilateral weighted average SUVR from a composite temporal meta-ROI (amygdala, entorhinal, fusiform, parahippocampal, inferior temporal, and middle temporal regions) was calculated based on FreeSurfer-parcellated regions as previously published [17–19]. A scan with a meta-ROI SUVR value >1.27 was considered T+, based on previously published data in an independent cohort from Gangnam Severance Hospital in Seoul, South Korea (threshold defined comparing Aβ + AD vs controls) [18].

T-status based on CSF PTau181—For binary T-status based on CSF PTau181, we derived a cutoff from an independent ADNI cohort with available results on the Elecsys Phospho-Tau (181P) assay. This was done by estimating a threshold comparing Aβ + AD subjects ($n = 183$) vs controls (independent of amyloid status, $n = 404$) with a receiver operating characteristic analysis, mirroring the methodology of the previously published threshold used for the temporal meta-ROI SUVR [18]. Using the Youden Index, a cutoff value of 24.5 pg/mL was found (sensitivity 0.70, specificity 0.84, area under the curve 0.83 (95% CI 0.80–0.87)).

Statistical analyses

For visual assessment of FTP, analysis of intra- and inter-rater agreement was performed using Cohen's kappa statistic. To evaluate concordance between PET-based and CSF-based T-status, overall percent agreement (OPA) was used. For evaluation of diagnostic performance by modality, accuracy in the study sample is provided, along with estimated area under the curve (AUC, calculated as sensitivity + specificity/2), to provide a metric that is not biased by the prevalence estimate in the sample. Between-group comparisons were performed using the Kruskal-Wallis H test for continuous variables and x^2 for nominal variables. Statistical significance was considered for $p < 0.05$. Statistical analyses were performed using SPSS (version 25, IBM, Armonk, NY).

Results

Patient characteristics can be found in Table 1. The cohort consisted of 127 cognitively normal (CN) participants, 106 MCI subjects, 84 AD_c patients, and 34 patients with non-AD disorders. There was a statistically significant difference in age, sex, education, MMSE, and rate of Aβ positivity between diagnostic groups. The distribution of CSF PTau181 and FTP SUVR by clinical diagnosis can be found in Supplementary Fig. 2.

Reliability of FTP visual assessment

Using the visual rating scheme for determination of binary T-status on FTP, intra-rater reliability ($n = 47$) for rater 1 was $\kappa = 0.87$ (95% CI 0.73–1.00) and for rater 2 was $\kappa = 0.78$ (95% CI 0.59–0.96). Overall percent agreement ($n = 351$) was 84%, with 57 cases requiring consensus read from the third rater (Supplementary Fig. 3). Inter-rater reliability in the overall sample was $\kappa = 0.64$ (95% CI 0.56–0.72), and $k = 0.79$ (95% CI 0.40–1.00) for scans of participants with AD_c.

T-status by modality and clinical diagnosis

Overall, FTP visual reads yielded the highest rates of T+ (Fig. 2). This was true across clinical diagnoses, and for Aβ + and Aβ − participants, with the exception of Aβ − non-AD dementia. T+ as defined by SUVR increased progressively from CN to MCI to AD_c and showed the lowest rates of T+ in Aβ − participants. T+ designation by CSF PTau181 was intermediate between FTP visual reads and SUVR values in CN, similar to SUVR in MCI, and lower in AD_c. CSF PTau181 generally yielded lower rates of T+ than FTP visual reads in Aβ − participants, and yielded zero T+ designations in the Aβ − AD_c category (likely clinical misdiagnosis of AD).

Concordance in T-status between modalities

Figure 3 shows four representative cases with discordance in T-status between at least one modality pair. These examples illustrate the potential advantage of integrating visual assessment of tau PET, which in early cases could detect subtle increased binding in a classic AD-like pattern, or significant binding outside of the target ROI, which were missed by SUVR quantification (first, second, and fourth rows in Fig. 3). The third case (Aβ−) illustrates false-positive near-threshold SUVR quantification, with non-AD binding pattern upon visual assessment (predominant binding in the frontal white matter), as we know that FTP may show subtle increased signal in cases with non-AD pathology [49–51].

status was concordant between all three modalities in 206 participants (59%). Overall percent agreement between modality pairs ranged from 68 to 76% in the whole cohort, with lowest overall agreement between FTP visual read and CSF PTau181 (Fig. 4). FTP SUVR and CSF PTau181 showed consistently high agreement in CN, MCI, and AD_c, whereas agreement between FTP SUVR and visual reads increased with clinical impairment and was nearly perfect (95%) in AD_c. In non-AD dementia, concordance was lowest between FTP SUVR and CSF pTau181. There was a significant positive correlation between continuous measures of CSF PTau181 and FTP SUVR ($r = 0.61$, $p < .001$; Fig. 5). Nearly all patients who were T+ on FTP SUVR were also T+ on visual assessment, while half of the patients

who were T+ on CSF PTau181 and T− on FTP SUVR quantification were T+ on visual assessment (Fig. 5, top left quadrant). Details of positive and negative percent agreement between modalities can be found in Supplementary Table 3.

Factors associated with a discordance in T-status

When comparing patients with concordant T-status across all three modalities to patients with discordance in at least one modality pair (Table 2), patients with a discordance in T-status were significantly older, were more likely to be male, and had intermediate rates of Aβ positivity, mean CSF PTau181 and FTP SUVR values. CN Aβ + participants were disproportionally represented in this group (67%) and were nearly always T+ on CSF and/or FTP visual assessment, while negative on SUVR quantification. In total, 27% of Aβ + AD_c patients were also found in this category, nearly all of whom were positive on both measures of tau PET but negative on CSF PTau181.

In subjects who had a discordant T-status in at least one modality pair, the mean CSF PTau181 and FTP SUVR values were very close to the cutoff used for binary classification. For visual assessment of FTP, cases requiring consensus from a third rater tended to have lower values of both CSF PTau181 (mean 20.7 pg/L) and FTP SUVR (mean 1.15) (Supplementary Fig. 4).

Focusing on patients with clinical diagnosis of AD ($n = 84$), there was no significant difference in global cognition (MMSE) between participants who were CSF T+ (~ 71%) and T− (~ 29%) ($p = .40$, Supplementary Table 4). Average FTP SUVR was higher in T+ CSF patients compared to T− ($p < 0.001$).

Sensitivity and specificity of T-status for Aβ + MCI/ADc by modality

To determine sensitivity and specificity of T-status obtained with each modality, we contrasted Aβ + cognitively impaired participants (MCI or AD_c) with all other subjects. Sensitivity was highest with FTP visual assessment (0.96, 95% CI 0.91–0.98), while specificity was highest with FTP SUVR quantification (0.91, 95% CI 0.87–0.95). CSF PTau181 had 0.73 sensitivity (95% CI 0.64–0.80) and 0.72 specificity (95% CI 0.65–0.78; Table 3). Overall accuracy was highest with FTP SUVR quantification (0.89, 95% CI 0.85–0.92, AUC 0.88), followed by FTP visual assessment (0.74, 95% CI 0.69–0.79, AUC 0.78) and CSF PTau181 (0.72, 95% CI 0.67–0.77, AUC 0.73).

When discriminating Aβ + vs Aβ − subjects regardless of clinical diagnosis or stage, overall accuracy was similar for FTP visual assessment and SUVR quantification (0.81, 95% CI 0.76–0.85, AUC 0.80 and 0.80, 95% CI 0.76–0.84, AUC 0.82 respectively), with nominally higher sensitivity for visual assessment (0.89, 95% CI 0.84–0.93), and higher specificity for SUVR quantification (0.96, 95% CI 0.92–0.99). CSF PTau181 showed intermediate sensitivity and specificity (0.66, 95% CI 0.59–0.73 and 0.79, 95% CI 0.72–0.85, overall accuracy 0.72, 95% CI 0.67–0.77, AUC 0.73). In early clinical disease stages (Aβ + CN and MCI participants), FTP visual assessment yielded highest sensitivity (71% and 90% respectively), compared with 21% and 70% for FTP SUVR quantification and 52% and 70% for CSF PTau181.

Autopsy was available in a subsample of 11 participants from the UCSF ADRC cohort (mean age at time of PET 63.9 years, mean PET to autopsy interval 2.7 years). Of the 11 patients, four had AD both clinically and at autopsy, five patients had non-AD disorders at autopsy, and the remaining two patients had mixed AD and non-AD pathology (supplementary Table 5). Using intermediate-to-high ADNC [52] as a gold standard, the highest overall accuracy was with FTP visual assessment (1.00, 95% CI 0.72–1.00, AUC 1.00), followed by FTP SUVR quantification (0.82, 95% CI 0.48–0.98, AUC 0.82) and CSF PTau181 (0.64, 95% CI 0.31–0.89, AUC 0.65). Using pathological neurofibrillary tangle Braak stage ≥ IV as a gold standard increased accuracy for CSF PTau181 (FTP visual assessment: 0.91, 95% CI 0.59–1.00, FTP SUVR quantification: 0.73, 95% CI 0.39–0.94, CSF PTau181: 0.73, 95% CI 0.39–0.94). Using a composite measure of CSF PTau181 and amyloid (PTau181/Aβ42 ratio > 0.028 [25]) also improved accuracy for detecting pathological Braak stage IV or higher (0.91, 95% CI 0.59–1.00).

Discussion

We compared CSF PTau181, visual assessment, and SUVR quantification of FTP to define T-status in a large sample of controls and patients with neurodegenerative diseases accrued via three distinct cohort studies. Overall, we found concordance between all three modalities in 59% of participants. T-status designation varied by both modality and disease stage. FTP visual reads showed the highest sensitivity but generally lower specificity, with many Aβ − cases designated as T+, especially in CN subjects. FTP SUVR showed highest specificity, but sensitivity was low in Aβ + CN, increasing progressively in MCI and dementia. Using our cutoff value, CSF PTau181 showed good specificity across disease stages, with high sensitivity in Aβ + CN but reaching a relative plateau in Aβ + MCI. Overall, our results support an emerging recognition that T-status is dependent on both the biomarker used (CSF vs PET) and the method of measurement. Each modality and method has strengths and weaknesses that should be considered in the design of studies employing tau biomarkers, and using a combination of biomarkers may be beneficial.

Although biomarkers of tau are used interchangeably in the AT(N) framework [7], CSF and PET do not necessarily reflect the same underlying pathological processes, and differences in the biological substrate of each modality could explain some of the discrepancies observed in our results. Specifically, CSF PTau181 may be measuring Aβ-induced changed in tau phosphorylation and secretion as measured in soluble species [27], while PET radiotracers bind to paired helical filaments of aggregated tau fibrils [53]. Additionally, FTP PET visual reads have been shown to reliably identify later stages of tau pathology (Braak stage V–VI) [22], and SUVR quantification may additionally allow detection of Braak stage IV [1, 54, 55]. CSF PTau181 has been proposed as an earlier marker of tau pathology [27], though correlations with autopsy studies are still pending.

Concordance of T-status derived from FTP visual assessment, SUVR quantification, and CSF PTau181 was moderate, averaging around 70–75% between modality pairs in the whole cohort. This is in line with previously published results on the concordance between FTP SUVR quantification and CSF PTau181, for example, 83% in a cohort from UCSF using the INNO-BIA AlzBio3 CSF Ptau181 assay [12], 65–77% in BioFINDER using

(EUROIMMUN and INNOTEST) [32], and 75% in a recent review of ADNI participants using the Elecsys Phospho-Tau (181P) assay [8].

The rates of T+ and agreement between tau biomarkers varied by disease stage. It has been hypothesized that CSF PTau181 becomes positive before tau PET, and may actually decrease in late stages of AD [3, 12, 56–58]. In contrast, FTP tracks disease progression in a linear way along disease course, which could explain discordance between the two biomarkers in advanced cases. Mattsson-Carlgren et al. found a higher percentage of T+ with CSF PTau181 compared to SUVR quantification in the inferior temporal cortex in cognitively unimpaired Aβ + subjects [32], and none had significant FTP signal in Braak regions V–VI [27]. This could explain the disproportionate number of T+ cases by CSF PTau181 and/or FTP visual assessment compared to SUVR quantification, which possibly represent early stages of the disease and may be subthreshold for quantification. In contrast, the near perfect agreement in T+ assignment between FTP visual assessment and SUVR quantification found in patients with AD_c is not surprising, given the high level of signal that is generally observed in these individuals [59, 60]. The concordance with CSF PTau181 was lower, however, with around 29% AD_c patients being T− on CSF. Similarly, Mattsson et al. had found that 46% of patients with AD dementia and positive tau PET had negative CSF PTau181 [14], although with a different assay. The lower concordance with CSF PTau181 in this patient group could be explained by differences in dynamics and longitudinal change of each modality. In our cohort, however, the AD_c T− CSF patients did not have lower MMSE to suggest that they represent more advanced cases.

Our results show that FTP visual assessment is a reliable tool for defining T-status in persons with cognitive impairment. Intra- and inter-rater reliability values in our study were similar to previously described visual rating schemes by Sonni et al. (in press) and Fleisher et al. [22]. Expertise and individual rater characteristics could certainly have influenced our results; for example, in this study, reads by rater 1 were more specific, while reads by rater 2 were more sensitive. Obtaining consensus by a third rater in discordant cases, however, should limit rater effect. In addition, the pattern of mild temporal binding remains of unknown significance. While we considered it to be T+, possibly reflecting early AD pathology, other groups consider binding restricted to the medial and/or anterior temporal lobes as T− [22]. The relatively high rate of T+ in Aβ − CN subjects in our study (34%) may therefore represent “over-reading” of mild temporal signal and/or noise. However, a higher proportion of Aβ + CN (71%) were visually read as T+, suggesting that there may be some visually discernable biologically meaningful signal. Further studies with histopathological correlation in cognitively unimpaired subjects would be needed to guide visual interpretation of mild temporal signal. Modifying our visual rating scheme to consider only advanced AD-like pattern of binding as T+ would likely increase specificity at the expense of sensitivity. Off-target binding, especially in the choroid plexus or at the base of the skull, may also lead to challenges in visual interpretation of the medial temporal lobe, which may limit specificity.

Our comparative accuracy analyses showed that sensitivity for detection of Aβ + MCI or AD patients can be maximized with FTP visual assessment; however, this method yielded a higher number of T+ in Aβ − participants. Focusing on the 34 Aβ − subjects who were T+

on visual assessment alone, all but one were CN individuals or MCI, and the vast majority were from the ADNI cohort. Qualitatively, these subjects' scans all displayed a similar pattern of FTP binding, consisting of mild signal especially in the temporal lobes. It is known that tau pathology may accumulate in the absence of Aβ in primary age-related tauopathy (PART) [61]. Other groups have also described increased FTP signal in cognitively unimpaired participants, predominantly in the medial temporal lobes [62]. It is possible that visual assessment of tau PET picks up mild elevation in FTP that is not specific to underlying AD pathology, including but not limited to PART. Limiting investigation with tau PET to those subjects that are cognitively impaired or Aβ+, in an attempt to limit false-positive visual reads, might be appropriate.

Previous studies have reported higher sensitivity with CSF PTau181 than with FTP SUVR quantification [8]. Sensitivity and specificity values for each modality are influenced by the threshold used for binary classification. The cutoff value we used for FTP SUVR has been previously validated [18] and is similar to those used in previous studies, with most thresholds for quantification of a temporal meta-ROI ranging from 1.2 to 1.4 SUVR [8, 17–19, 32]. Our CSF PTau181 cutoff was similar to previously published threshold with the Elecsys Phospho-Tau (181P) electrochemiluminescence immunoassay in a cohort of ADNI subjects (26.64 pg/mL), though using a different gold standard (Aβ − cognitively unimpaired controls vs Aβ + AD subjects) [8] and to a proposed cutoff value of 27 pg/mL to predict cognitive decline [63]. The threshold we used was also similar to the 95th percentile of CSF PTau181 in CN Aβ − in the independent ADNI cohort from which our cutoff was derived (29.89 pg/mL, $n = 271$). Given the distribution of CSF PTau181 and FTP SUVR values in patients with discordant T-status, we can hypothesize that near-threshold cases explain a significant proportion of disagreement between modalities. Differences in sensitivity of CSF PTau181 might also be attributed to cohort composition. For example, in the study by Meyer et al., there was a high number of cognitively unimpaired subjects ($n = 214$) and few AD dementia patients ($n = 11$). Finally, some authors have suggested using a ratio of PTau181 to Aβ42 (to detect Aβ + subjects) [25], which in our subsample of 11 patients with autopsy-confirmed diagnosis, led to a higher accuracy of CSF PTau181 for detecting AD. However, we opted not to use this ratio for comparative analyses of T-status, since Aβ42 reflects underlying amyloid pathology and could not be directly compared to measures of tau PET alone.

Recent advances have been reported in the development and validation of plasma assays for PTau181 and PTau217 [64–68]. Plasma measures capture soluble phosphorylated tau species that have crossed the blood-brain barrier and correlate with CSF PTau concentrations and tau PET signal. Early data support the notion that plasma PTau follows the trajectory of CSF PTau, changing in the preclinical disease stage in association with Aβ, and reaching a relative plateau in the early symptomatic stage [68–71]. Future work will determine how plasma measures of amyloid, tau, and neurodegeneration compare to CSF and imaging markers in implementation of AT(N) classification in the AD Research Framework [7].

Major strengths of this study include the large number of subjects recruited from three different studies and spanning a wide range of neurodegenerative conditions, and the direct comparison of both visual and quantitative tau PET with CSF PTau measures. Furthermore,

we had autopsy diagnosis available in a small subsample. Our study has several limitations. First, there were methodological differences between the three studies, notably in the composition of the cohorts, method of determination of amyloid status, and pre-analytic handling of CSF samples. Second, we used a visual interpretation method that was developed in-house—our method is similar but not identical to the method that has recently been validated, in particular regarding signal restricted to the anterio-medial temporal lobes [22]. Third, our results cannot be generalized to other tau PET tracers or CSF tau assays than the ones used in our study. Performance of both visual ratings and SUVR quantification of second-generation compounds such as MK-6240, JNJ-067, or RO-948 [16] may differ from FTP-PET. Similarly, CSF assays using different phosphorylation sites, for example, PTau217, which has been shown to have high correlation with FTP [65], may yield different estimates of accuracy and inter-modality concordance.

Conclusion

Biomarkers of tau, as listed in the AT(N) framework, are not interchangeable and show variable concordance depending on method of analysis and cohort. In our study, concordance of T-status derived from FTP visual assessment, SUVR quantification, and CSF PTau181 varied across disease stage. An FTP visual read scheme that includes mild temporal binding maximizes sensitivity to early disease stage, including in preclinical AD, while SUVR quantification maximizes specificity. CSF PTau181 shows balanced sensitivity and specificity across the AD continuum. Each modality may offer a complementary role, and a combination of approaches may be ultimately beneficial. Recently published work has suggested measuring T as a continuous rather than binary variable may correlate better with prognosis [32]. Further work will be needed to compare FTP visual assessment and SUVR quantification to novel plasma biomarkers of phosphorylated tau [24, 64, 68].

Supplementary Material

Refer to Web version on PubMed Central for supplementary material.

Acknowledgments

We would like to acknowledge all patients and caregivers for their time and participation in this study.

Funding This study was supported by the National Institute on Aging grants (P30-AG062422 to B.L.M and G.D.R., P01-AG019724 to B.L.M., R01-AG-045611 to G.D.R.), Alzheimer's Association (AARF-16-443577 to R.L.J., AACSF-19-617663 to D.N.S.-M.), and Rainwater Charitable Foundation (Tau Consortium) (to G.D.R. and W.J.J.). Avid Radiopharmaceuticals enabled use of the Flortaucipir tracer, and Roche Diagnostics provided the Elecsys kits for CSF analysis; Avid Radiopharmaceuticals and Roche Diagnostics did not provide direct funding and was not involved in data analysis or interpretation. COBAS, COBAS E, and ELECSYS are trademarks of Roche. Data collection and sharing for this project was funded by the Alzheimer's Disease Neuroimaging Initiative (ADNI) (National Institutes of Health Grant U01 AG024904) and DOD ADNI (Department of Defense award number W81XWH-12-2-0012). ADNI is funded by the National Institute on Aging, the National Institute of Biomedical Imaging and Bioengineering, and through generous contributions from the following: AbbVie, Alzheimer's Association; Alzheimer's Drug Discovery Foundation; Araclon Biotech; BioClinica, Inc.; Biogen; Bristol-Myers Squibb Company; CereSpir, Inc.; Cogstate; Eisai Inc.; Elan Pharmaceuticals, Inc.; Eli Lilly and Company; EuroImmun; F. Hoffmann-La Roche Ltd. and its affiliated company Genentech, Inc.; Fujirebio; GE Healthcare; IXICO Ltd.; Janssen Alzheimer Immunotherapy Research & Development, LLC.; Johnson & Johnson Pharmaceutical Research & Development LLC.; Lumosity; Lundbeck; Merck & Co., Inc.; Meso Scale Diagnostics, LLC.; NeuroRx Research; Neurotrack Technologies; Novartis Pharmaceuticals Corporation; Pfizer Inc.; Piramal Imaging; Servier; Takeda Pharmaceutical Company; and Transition Therapeutics. The Canadian Institutes of Health

Research is providing funds to support ADNI clinical sites in Canada. Private sector contributions are facilitated by the Foundation for the National Institutes of Health (www.fnih.org). The grantee organization is the Northern California Institute for Research and Education, and the study is coordinated by the Alzheimer's Therapeutic Research Institute at the University of Southern California. ADNI data are disseminated by the Laboratory for Neuro Imaging at the University of Southern California.

References

1. Lowe VJ, Curran G, Fang P, Liesinger AM, Josephs KA, Parisi JE, et al. An autoradiographic evaluation of AV-1451 tau PET in dementia. Acta Neuropathol Commun. 2016;4:58. 10.1186/s40478-016-0315-6. [PubMed: 27296779]
2. Marquie M, Normandin MD, Vanderburg CR, Costantino IM, Bien EA, Rycyna LG, et al. Validating novel tau positron emission tomography tracer [F-18]-AV-1451 (T807) on postmortem brain tissue. Ann Neurol. 2015;78:787–800. 10.1002/ana.24517. [PubMed: 26344059]
3. Scholl M, Maass A, Mattsson N, Ashton NJ, Blennow K, Zetterberg H, et al. Biomarkers for tau pathology. Mol Cell Neurosci. 2019;97:18–33. 10.1016/j.mcn.2018.12.001. [PubMed: 30529601]
4. Olsson B, Lautner R, Andreasson U, Ohrfelt A, Portelius E, Bjerke M, et al. CSF and blood biomarkers forthe diagnosis of Alzheimer's disease: a systematic review and meta-analysis. Lancet Neurol. 2016;15:673–84. 10.1016/S1474-4422(16)00070-3. [PubMed: 27068280]
5. Cummings J The National Institute on Aging-Alzheimer's association framework on Alzheimer's disease: application to clinical trials. Alzheimers Dement. 2019;15:172–8. 10.1016/j.jalz.2018.05.006. [PubMed: 29936146]
6. Blennow K, Zetterberg H. Biomarkers for Alzheimer's disease: current status and prospects for the future. J Intern Med. 2018;284:643–63. 10.1111/joim.12816. [PubMed: 30051512]
7. Jack CR Jr, Bennett DA, Blennow K, Carrillo MC, Feldman HH, Frisoni GB, et al. A/T/N: an unbiased descriptive classification scheme for Alzheimer disease biomarkers. Neurology. 2016;87:539–47. 10.1212/WNL.0000000000002923. [PubMed: 27371494]
8. Meyer PF, Binette AP, Gonneaud J, Breitner JCS, Villeneuve S. Characterization of Alzheimer disease biomarker discrepancies using cerebrospinal fluid phosphorylated tau and AV1451 positron emission tomography. JAMA Neurol. 2020. 10.1001/jamaneurol.2019.4749.
9. Chhatwal JP, Schultz AP, Marshall GA, Boot B, Gomez-Isla T, Dumurgier J, et al. Temporal T807 binding correlates with CSF tau and phospho-tau in normal elderly. Neurology. 2016;87:920–6. 10.1212/WNL.0000000000003050. [PubMed: 27473132]
10. Gordon BA, Friedrichsen K, Brier M, Blazey T, Su Y, Christensen J, et al. The relationship between cerebrospinal fluid markers of Alzheimer pathology and positron emission tomography tau imaging. Brain. 2016;139:2249–60. 10.1093/brain/aww139. [PubMed: 27286736]
11. Brier MR, Gordon B, Friedrichsen K, McCarthy J, Stern A, Christensen J, et al. Tau and Abeta imaging, CSF measures, and cognition in Alzheimer's disease. Sci Transl Med. 2016;8:338ra66. 10.1126/scitranslmed.aaf2362.
12. La Joie R, Bejanin A, Fagan AM, Ayakta N, Baker SL, Bourakova V, et al. Associations between [(18)F]AV1451 tau PET and CSF measures of tau pathology in a clinical sample. Neurology. 2018;90:e282–e90. 10.1212/WNL.0000000000004860. [PubMed: 29282337]
13. Mattsson N, Smith R, Strandberg O, Palmqvist S, Scholl M, Insel PS, et al. Comparing (18)F-AV-1451 with CSF t-tau and p-tau for diagnosis of Alzheimer disease. Neurology. 2018;90:e388–e95. 10.1212/WNL.0000000000004887. [PubMed: 29321235]
14. Mattsson N, Scholl M, Strandberg O, Smith R, Palmqvist S, Insel PS, et al. (18)F-AV-1451 and CSF T-tau and P-tau as biomarkers in Alzheimer's disease. EMBO Mol Med. 2017;9:1212–23. 10.15252/emmm.201707809. [PubMed: 28743782]
15. Zhao Q, Liu M, Ha L, Zhou Y, Alzheimer's disease neuroimaging I. Quantitative (18)F-AV1451 brain Tau PET imaging in cognitively normal older adults, mild cognitive impairment, and Alzheimer's disease patients. Front Neurol. 2019;10:486. doi:10.3389/fneur.2019.00486. [PubMed: 31156534]
16. Leuzy A, Chiotis K, Lemoine L, Gillberg PG, Almkvist O, Rodriguez-Vieitez E, et al. Tau PET imaging in neurodegenerative tauopathies-still a challenge. Mol Psychiatry. 2019;24:1112–34. 10.1038/s41380-018-0342-8. [PubMed: 30635637]

17. Jack CR Jr, Wiste HJ, Weigand SD, Therneau TM, Lowe VJ, Knopman DS, et al. Defining imaging biomarker cut points for brain aging and Alzheimer's disease. Alzheimers Dement. 2017;13:205–16. 10.1016/j.jalz.2016.08.005. [PubMed: 27697430]

18. Ossenkoppele R, Rabinovici GD, Smith R, Cho H, Scholl M, Strandberg O, et al. Discriminative accuracy of [18F]flortaucipir positron emission tomography for Alzheimer disease vs other neurodegenerative disorders. JAMA. 2018;320:1151–62. 10.1001/jama.2018.12917. [PubMed: 30326496]

19. Maass A, Landau S, Baker SL, Horng A, Lockhart SN, La Joie R, et al. Comparison of multiple tau-PET measures as biomarkers in aging and Alzheimer's disease. Neuroimage. 2017;157:448–63. 10.1016/j.neuroimage.2017.05.058. [PubMed: 28587897]

20. Jack CR Jr, Therneau TM, Weigand SD, Wiste HJ, Knopman DS, Vemuri P, et al. Prevalence of biologically vs clinically defined Alzheimer spectrum entities using the National Institute on Aging-Alzheimer's association research framework. JAMA Neurol. 2019. 10.1001/jamaneurol.2019.1971.

21. Baker SL, Harrison TM, Maass A, La Joie R, Jagust W. Effect of off-target binding on (18)F-flortaucipir variability in healthy conrols across the lifespan. J Nucl Med. 2019. 10.2967/jnumed.118.224113.

22. Fleisher AS, Pontecorvo MJ, Devous MD Sr, Lu M, Arora AK, Truocchio SP, et al. Positron emission tomography imaging with [18F]flortaucipir and postmortem assessment of Alzheimer disease neuropathologic changes. JAMA Neurol. 2020. 10.1001/jamaneurol.2020.0528.

23. Blennow K, Hampel H, Weiner M, Zetterberg H. Cerebrospinal fluid and plasma biomarkers in Alzheimer disease. Nat Rev Neurol. 2010;6:131–44. 10.1038/nrneurol.2010.4. [PubMed: 20157306]

24. Palmqvist S, Janelidze S, Stomrud E, Zetterberg H, Karl J, Zink K, et al. Performance of fully automated plasma assays as screening tests for Alzheimer disease-related beta-amyloid status. JAMA Neurol. 2019. 10.1001/jamaneurol.2019.1632.

25. Hansson O, Seibyl J, Stomrud E, Zetterberg H, Trojanowski JQ, Bittner T, et al. CSF biomarkers of Alzheimer's disease concord with amyloid-beta PET and predict clinical progression: a study of fully automated immunoassays in BioFINDER and ADNI cohorts. Alzheimers Dement. 2018;14:1470–81. 10.1016/j.jalz.2018.01.010. [PubMed: 29499171]

26. Lifke V, Kollmorgen G, Manuilova E, Oelschlaegel T, Hillringhaus L, Widmann M, et al. Elecsys((R)) Total-tau and phospho-tau (181P) CSF assays: analytical performance of the novel, fully automated immunoassays for quantification of tau proteins in human cerebrospinal fluid. Clin Biochem. 2019. doi:10.1016/j.clinbiochem.2019.05.005.

27. Mattsson-Carlgren N, Andersson E, Janelidze S, Ossenkoppele R, Insel P, Strandberg O, et al. Abeta deposition is associated with increases in soluble and phosphorylated tau that precede a positive Tau PET in Alzheimer's disease. Sci Adv. 2020;6:eaaz2387. doi:10.1126/sciadv.aaz2387. [PubMed: 32426454]

28. Blennow K, Mattsson N, Scholl M, Hansson O, Zetterberg H. Amyloid biomarkers in Alzheimer's disease. Trends Pharmacol Sci. 2015;36:297–309. 10.1016/j.tips.2015.03.002. [PubMed: 25840462]

29. Fagan AM, Mintun MA, Mach RH, Lee SY, Dence CS, Shah AR, et al. Inverse relation between in vivo amyloid imaging load and cerebrospinal fluid Abeta42 in humans. Ann Neurol. 2006;59:512–9. 10.1002/ana.20730. [PubMed: 16372280]

30. Doecke JD, Ward L, Burnham SC, Villemagne VL, Li QX, Collins S, et al. Elecsys CSF biomarker immunoassays demonstrate concordance with amyloid-PET imaging. Alzheimers Res Ther. 2020;12:36. 10.1186/s13195-020-00595-5. [PubMed: 32234072]

31. Oh M, Kim JS, Oh JS, Lee CS, Chung SJ. Different subregional metabolism patterns in patients with cerebellar ataxia by 18F-fluorodeoxyglucose positron emission tomography. PLoS One. 2017;12:e0173275. 10.1371/journal.pone.0173275. [PubMed: 28319124]

32. Mattsson-Carlgren N, Leuzy A, Janelidze S, Palmqvist S, Stomrud E, Strandberg O, et al. The implications of different approaches to define AT(N) in Alzheimer disease. Neurology. 2020. 10.1212/WNL.0000000000009485.

33. Okafor M, Nye JA, Shokouhi M, Shaw LM, Goldstein F, Hajjar I. 18F-Flortaucipir PET associations with cerebrospinal fluid, cognition, and neuroimaging in mild cognitive impairment due to Alzheimer's disease. J Alzheimers Dis. 2020;74:589–601. 10.3233/JAD-191330. [PubMed: 32065800]
34. Wolters EE, Ossenkoppele R, Verfaillie SCJ, Coomans EM, Timmers T, Visser D, et al. Regional [(18)F]flortaucipir PET is more closely associated with disease severity than CSF p-tau in Alzheimer's disease. Eur J Nucl Med Mol Imaging. 2020. 10.1007/s00259-020-04758-2.
35. Albert MS, DeKosky ST, Dickson D, Dubois B, Feldman HH, Fox NC, et al. The diagnosis of mild cognitive impairment due to Alzheimer's disease: recommendations from the National Institute on Aging-Alzheimer's association workgroups on diagnostic guidelines for Alzheimer's disease. Alzheimers Dement. 2011;7: 270–9. 10.1016/j.jalz.2011.03.008. [PubMed: 21514249]
36. McKhann GM, Knopman DS, Chertkow H, Hyman BT, Jack CR Jr, Kawas CH, et al. The diagnosis of dementia due to Alzheimer's disease: recommendations from the National Institute on Aging-Alzheimer's association workgroups on diagnostic guidelines for Alzheimer's disease. Alzheimers Dement. 2011;7:263–9. 10.1016/j.jalz.2011.03.005. [PubMed: 21514250]
37. Rascovsky K, Hodges JR, Knopman D, Mendez MF, Kramer JH, Neuhaus J, et al. Sensitivity of revised diagnostic criteria for the behavioural variant of frontotemporal dementia. Brain. 2011;134: 2456–77. 10.1093/brain/awr179. [PubMed: 21810890]
38. Gorno-Tempini ML, Hillis AE, Weintraub S, Kertesz A, Mendez M, Cappa SF, et al. Classification of primary progressive aphasia and its variants. Neurology. 2011;76:1006–14. 10.1212/WNL.0b013e31821103e6. [PubMed: 21325651]
39. Armstrong MJ, Litvan I, Lang AE, Bak TH, Bhatia KP, Borroni B, et al. Criteria for the diagnosis of corticobasal degeneration. Neurology. 2013;80:496–503. 10.1212/WNL.0b013e31827f0fd1. [PubMed: 23359374]
40. Litvan I, Agid Y, Calne D, Campbell G, Dubois B, Duvoisin RC, et al. Clinical research criteria for the diagnosis of progressive supranuclear palsy (Steele-Richardson-Olszewski syndrome): report of the NINDS-SPSP international workshop. Neurology. 1996;47:1–9. 10.1212/wnl.47.1.1. [PubMed: 8710059]
41. Hoglinger GU, Respondek G, Stamelou M, Kurz C, Josephs KA, Lang AE, et al. Clinical diagnosis of progressive supranuclear palsy: the Movement Disorder Society criteria. Mov Disord. 2017;32:853–64. 10.1002/mds.26987. [PubMed: 28467028]
42. McKeith IG, Boeve BF, Dickson DW, Halliday G, Taylor JP, Weintraub D, et al. Diagnosis and management of dementia with Lewy bodies: fourth consensus report of the DLB consortium. Neurology. 2017;89:88–100. 10.1212/WNL.0000000000004058. [PubMed: 28592453]
43. Roman GC, Tatemichi TK, Erkinjuntti T, Cummings JL, Masdeu JC, Garcia JH, et al. Vascular dementia: diagnostic criteria for research studies. Report of the NINDS-AIREN international workshop. Neurology. 1993;43:250–60. 10.1212/wnl.43.2.250. [PubMed: 8094895]
44. Baker SL, Maass A, Jagust WJ. Considerations and code for partial volume correcting [(18)F]-AV-1451 tau PET data. Data Brief. 2017;15:648–57. 10.1016/j.dib.2017.10.024. [PubMed: 29124088]
45. Bittner T, Zetterberg H, Teunissen CE, Ostlund RE Jr, Militello M, Andreasson U, et al. Technical performance of a novel, fully automated electrochemiluminescence immunoassay for the quantitation of beta-amyloid (1-42) in human cerebrospinal fluid. Alzheimers Dement. 2016;12:517–26. 10.1016/j.jalz.2015.09.009. [PubMed: 26555316]
46. Sonni I, Lesman Segev OH, Baker SL, Iaccarino L, Korman D, Rabinovici GD, et al. Evaluation of a visual interpretation method for tau-PET with 18F-flortaucipir. Alzheimers Dement (Amst). 2020;12(1):e12133. 10.1002/dad2.12133. [PubMed: 33313377]
47. Braak H, Braak E. Neuropathological stageing of Alzheimer-related changes. Acta Neuropathol. 1991;82:239–59. 10.1007/BF00308809. [PubMed: 1759558]
48. Schwarz AJ, Yu P, Miller BB, Shcherbinin S, Dickson J, Navitsky M, et al. Regional profiles of the candidate tau PET ligand 18F-AV-1451 recapitulate key features of Braak histopathological stages. Brain. 2016;139:1539–50. 10.1093/brain/aww023. [PubMed: 26936940]

49. Tsai RM, Bejanin A, Lesman-Segev O, LaJoie R, Visani A, Bourakova V, et al. (18)F-Flortaucipir (AV-1451) tau PET in frontotemporal dementia syndromes. Alzheimers Res Ther. 2019;11:13. 10.1186/s13195-019-0470-7. [PubMed: 30704514]
50. Utianski RL, Whitwell JL, Schwarz CG, Senjem ML, Tosakulwong N, Duffy JR, et al. Tau-PET imaging with [18F]AV-1451 in primary progressive apraxia of speech. Cortex. 2018;99:358–74. 10.1016/j.cortex.2017.12.021. [PubMed: 29353121]
51. Josephs KA, Whitwell JL, Tacik P, Duffy JR, Senjem ML, Tosakulwong N, et al. [18F]AV-1451 tau-PET uptake does correlate with quantitatively measured 4R-tau burden in autopsy-confirmed corticobasal degeneration. Acta Neuropathol. 2016;132:931–3. 10.1007/s00401-016-1618-1. [PubMed: 27645292]
52. Montine TJ, Phelps CH, Beach TG, Bigio EH, Cairns NJ, Dickson DW, et al. National Institute on Aging-Alzheimer's association guidelines for the neuropathologic assessment of Alzheimer's disease: a practical approach. Acta Neuropathol. 2012;123:1–11. 10.1007/s00401-011-0910-3. [PubMed: 22101365]
53. Buerger K, Ewers M, Pirttila T, Zinkowski R, Alafuzoff I, Teipel SJ, et al. CSF phosphorylated tau protein correlates with neocortical neurofibrillary pathology in Alzheimer's disease. Brain. 2006;129:3035–41. 10.1093/brain/awl269. [PubMed: 17012293]
54. Pontecorvo MJ, Keene CD, Beach TG, Montine TJ, Arora AK, Devous MD Sr, et al. Comparison of regional flortaucipir PET with quantitative tau immunohistochemistry in three subjects with Alzheimer's disease pathology: a clinicopathological study. EJNMMI Res. 2020;10:65. 10.1186/s13550-020-00653-x. [PubMed: 32542468]
55. Soleimani-Meigooni DN, Iaccarino L, La Joie R, Baker S, Bourakova V, Boxer AL, et al. 18F-Flortaucipir PET to autopsy comparisons in Alzheimer's disease and other neurodegenerative diseases. Brain. 2020. 10.1093/brain/awaa276.
56. Toledo JB, Xie SX, Trojanowski JQ, Shaw LM. Longitudinal change in CSF tau and Abeta biomarkers for up to 48 months in ADNI. Acta Neuropathol. 2013;126:659–70. 10.1007/s00401-013-1151-4. [PubMed: 23812320]
57. Fagan AM, Xiong C, Jasielec MS, Bateman RJ, Goate AM, Benzinger TL, et al. Longitudinal change in CSF biomarkers in autosomal-dominant Alzheimer's disease. Sci Transl Med. 2014;6:226ra30. 10.1126/scitranslmed.3007901.
58. Leuzy A, Cicognola C, Chiotis K, Saint-Aubert L, Lemoine L, Andreasen N, et al. Longitudinal tau and metabolic PET imaging in relation to novel CSF tau measures in Alzheimer's disease. Eur J Nucl Med Mol Imaging. 2019;46:1152–63. 10.1007/s00259-018-4242-6. [PubMed: 30610252]
59. Ossenkoppele R, Schonhaut DR, Scholl M, Lockhart SN, Ayakta N, Baker SL, et al. Tau PET patterns mirror clinical and neuroanatomical variability in Alzheimer's disease. Brain. 2016;139:1551–67. 10.1093/brain/aww027. [PubMed: 26962052]
60. Scholl M, Ossenkoppele R, Strandberg O, Palmqvist S, Fs SB, Jogi J, et al. Distinct 18F-AV-1451 tau PET retention patterns in early-and late-onset Alzheimer's disease. Brain. 2017;140:2286–94. 10.1093/brain/awx171. [PubMed: 29050382]
61. Crary JF, Trojanowski JQ, Schneider JA, Abisambra JF, Abner EL, Alafuzoff I, et al. Primary age-related tauopathy (PART): a common pathology associated with human aging. Acta Neuropathol. 2014;128:755–66. 10.1007/s00401-014-1349-0. [PubMed: 25348064]
62. Lowe VJ, Bruinsma TJ, Min HK, Lundt ES, Fang P, Senjem ML, et al. Elevated medial temporal lobe and pervasive brain tau-PET signal in normal participants. Alzheimers Dement (Amst). 2018;10:210–6. 10.1016/j.dadm.2018.01.005. [PubMed: 29780865]
63. Blennow K, Shaw LM, Stomrud E, Mattsson N, Toledo JB, Buck K, et al. Predicting clinical decline and conversion to Alzheimer's disease or dementia using novel Elecsys Abeta(1-42), pTau and tTau CSF immunoassays. Sci Rep. 2019;9:19024. 10.1038/s41598-019-54204-z. [PubMed: 31836810]
64. Thijssen EH, La Joie R, Wolf A, Strom A, Wang P, Iaccarino L, et al. Diagnostic value of plasma phosphorylated tau181 in Alzheimer's disease and frontotemporal lobar degeneration. Nat Med. 2020;26:387–97. 10.1038/s41591-020-0762-2. [PubMed: 32123386]

65. Janelidze S, Stomrud E, Smith R, Palmqvist S, Mattsson N, Airey DC, et al. Cerebrospinal fluid p-tau217 performs better than p-tau181 as a biomarker of Alzheimer's disease. Nat Commun. 2020;11:1683. 10.1038/s41467-020-15436-0. [PubMed: 32246036]

66. Palmqvist S, Janelidze S, Quiroz YT, Zetterberg H, Lopera F, Stomrud E, et al. Discriminative accuracy of plasma phospho-tau217 for Alzheimer disease vs other neurodegenerative disorders. JAMA. 2020. 10.1001/jama.2020.12134.

67. Barthelemy NR, Horie K, Sato C, Bateman RJ. Blood plasma phosphorylated-tau isoforms track CNS change in Alzheimer's disease. J Exp Med. 2020;217. 10.1084/jem.20200861.

68. Karikari TK, Pascoal TA, Ashton NJ, Janelidze S, Benedet AL, Rodriguez JL, et al. Blood phosphorylated tau 181 as a biomarker for Alzheimer's disease: a diagnostic performance and prediction modelling study using data from four prospective cohorts. Lancet Neurol. 2020;19:422–33. 10.1016/S1474-4422(20)30071-5. [PubMed: 32333900]

69. Janelidze S, Mattsson N, Stomrud E, Lindberg O, Palmqvist S, Zetterberg H, et al. CSF biomarkers of neuroinflammation and cerebrovascular dysfunction in early Alzheimer disease. Neurology. 2018;91:e867–e77. 10.1212/WNL.0000000000006082. [PubMed: 30054439]

70. O'Connor A, Karikari TK, Poole T, Ashton NJ, Lantero Rodriguez J, Khatun A, et al. Plasma phospho-tau181 in presymptomatic and symptomatic familial Alzheimer's disease: a longitudinal cohort study. Mol Psychiatry. 2020. 10.1038/s41380-020-0838-x.

71. Lantero Rodriguez J, Karikari TK, Suarez-Calvet M, Troakes C, King A, Emersic A, et al. Plasma p-tau181 accurately predicts Alzheimer's disease pathology at least 8 years prior to postmortem and improves the clinical characterisation of cognitive decline. Acta Neuropathol. 2020. 10.1007/s00401-020-02195-x.

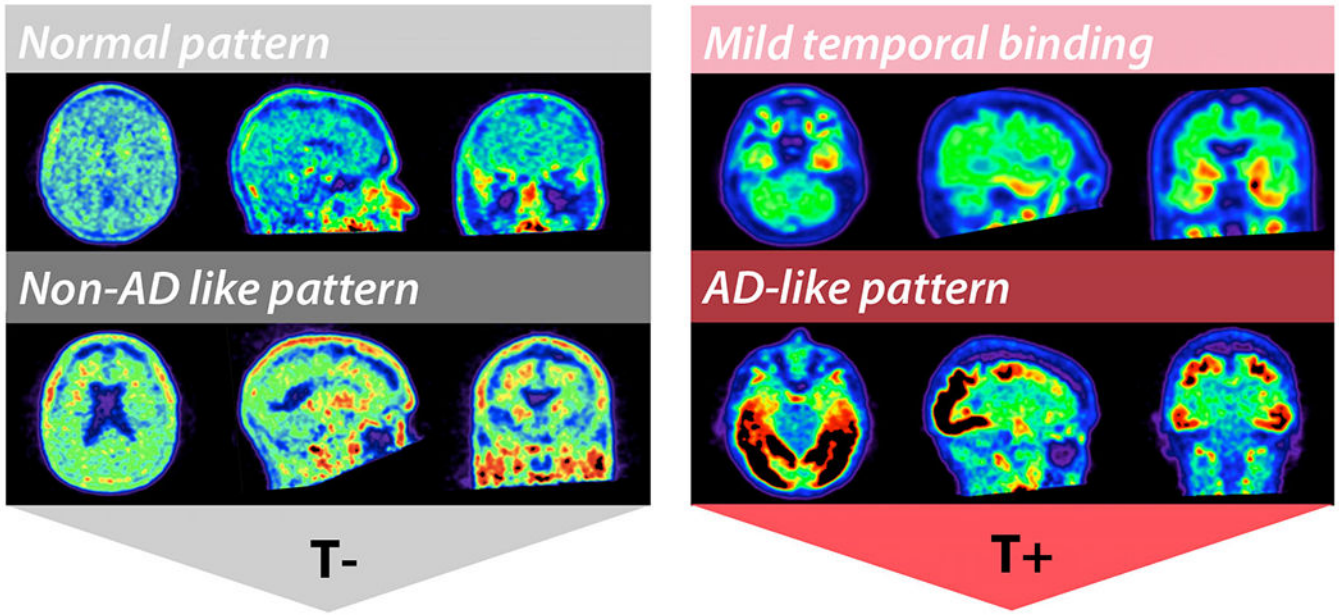

Fig. 1.

Rating scheme for visual assessment of FTP pattern of binding to define T-status. Normal pattern of binding and non-AD-like pattern (for example, mild-to-moderate signal in the frontal white matter) were assigned T-status. Classic AD-like pattern following Braak and Braak distribution extending beyond the temporal lobes, and mild temporal binding (confluent binding restricted to the temporal lobes) were assigned T+ status

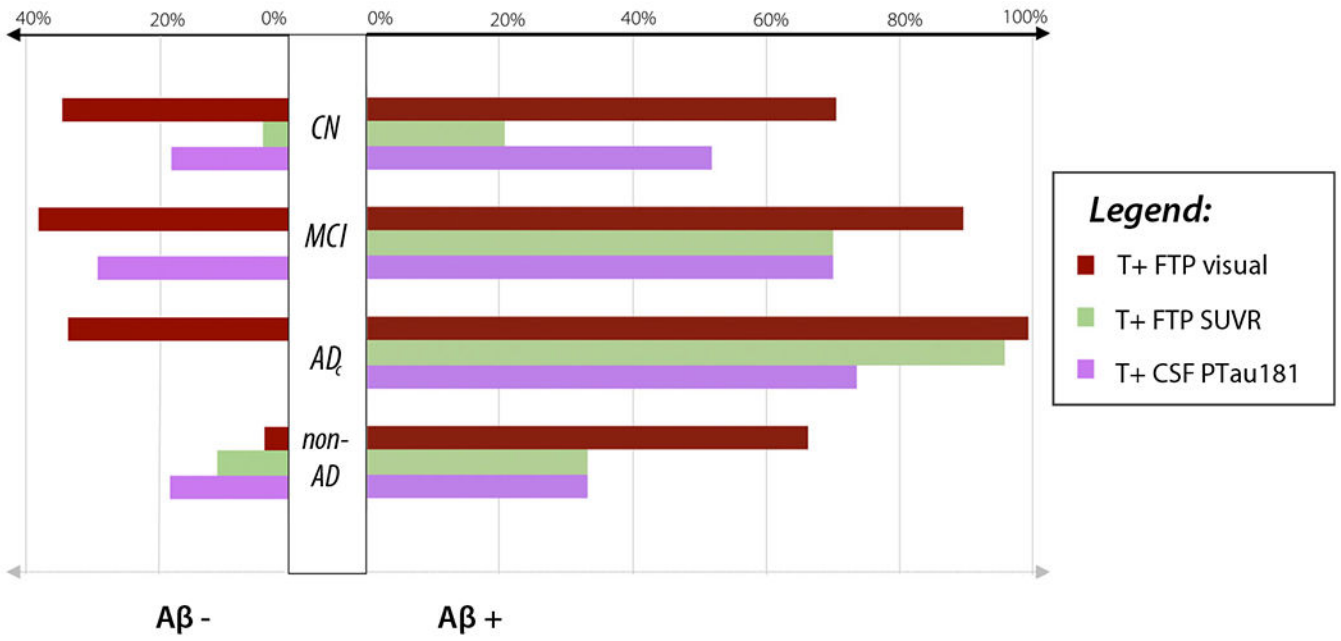

Fig. 2.

Percentage of T+ by modality, clinical diagnosis, and amyloid status. CN, cognitively normal; MCI, mild cognitive impairment; AD_c, Alzheimer's disease dementia; non-AD, non-AD disorders

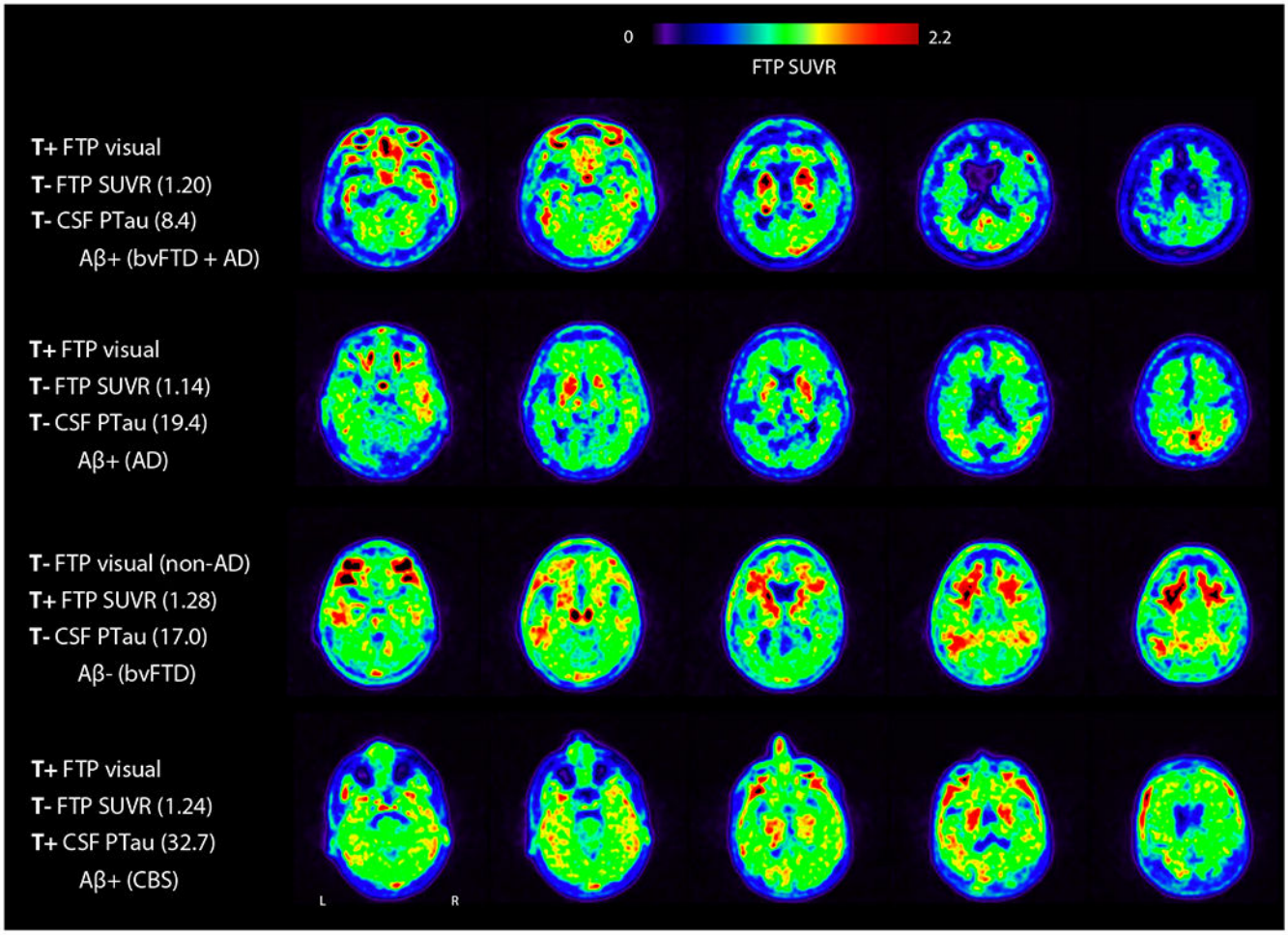

Fig. 3.

Examples of discordant T-status between FTP visual assessment, SUVR quantification, and CSF PTau181. Selected axial slices of FTP are shown. Amyloid status is based on PET. Clinical diagnosis is indicated in parentheses. bvFTD, behavioral variant frontotemporal dementia; CBS, corticobasal syndrome

Fig. 4.

Inter-modality overall percent agreement between modalities by clinical diagnosis. CN, cognitively normal; MCI, mild cognitive impairment; AD_c, Alzheimer's disease dementia; non-AD, non-AD disorders

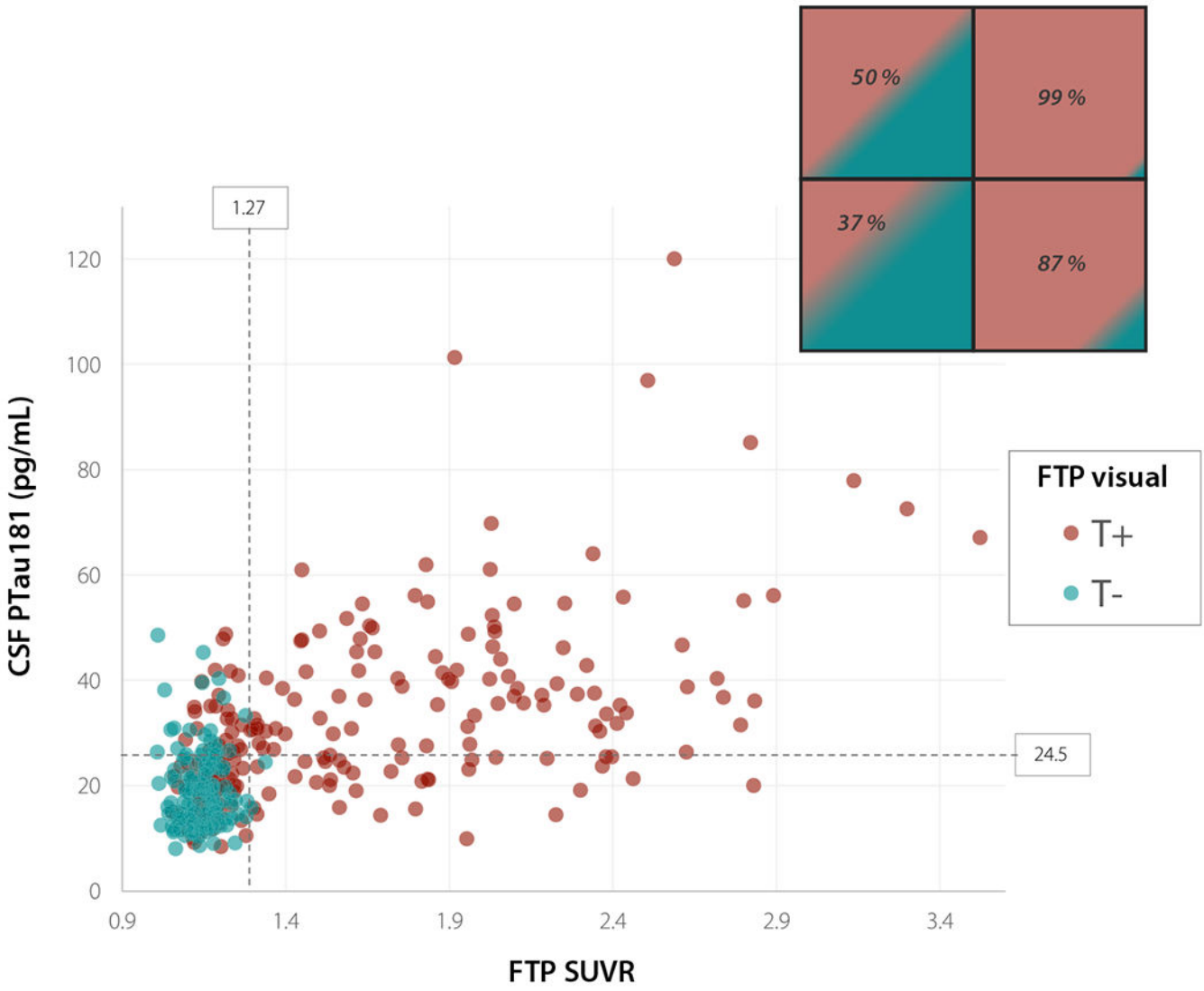

Fig. 5.

Scatterplot of CSF PTau181 and FTP SUVR values in T+ and T− patients by FTP visual assessment. Dotted lines show threshold of positivity for CSF PTau181 and FTP temporal meta-ROI SUVR. Insert in the top right corner shows percentage of T+ cases by visual assessment for each quadrant of the scatterplot

Table 1

Patient characteristics (n = 351). Mean ± SD is indicated for continuous variables

	CN (n = 127)	MCI (n = 106)	AD_c (n = 84)	Non-AD (n = 34)	p value
Age	73.9 ± 6.8	71.7 ± 9.0	66.1 ± 9.2	65.3 ± 9.7	$p \leq .001^{\dagger}$
Sex (M, %)	45 (35%)	47 (44%)	44 (52%)	20 (59%)	$p = .03$
Education	14.9 ± 3.8	15.8 ± 3.0	15.5 ± 3.5	17.4 ± 4.2	$p = .004^{\dagger\dagger}$
MMSE	29.2 ± 1.0	27.0 ± 2.7	20.9 ± 4.8	25.2 ± 6.3	$p < .001^{\dagger\dagger\dagger}$
Amyloid status (Aβ+, %)	48 (38%)	61 (58%)	81 (96%)	6 (18%)	$p < .001$
Provenance	UCSF ADRC 0	UCSF ADRC 15	UCSF ADRC 50	UCSF ADRC 33	
	ADNI 80	ADNI 83	ADNI 16	ADNI 0	
	BioFINDER 47	BioFINDER 8	BioFINDER 18	BioFINDER 1	

CN cognitively normal, *MCI* mild cognitive impairment, AD_C Alzheimer's disease dementia, *non-*AD_C non-AD disorders (including patients with clinical diagnoses of behavioral variant frontotemporal dementia, non-fluent variant primary progressive aphasia, progressive supranuclear palsy, corticobasal syndrome, dementia with Lewy bodies, and one subject with chronic traumatic encephalopathy)

†Significant for all pairwise comparisons except CN vs MCI (p = .26) and AD vs non-AD (p = 1.00)

††Pairwise comparisons significant only between CN and non-AD (p = .002)

†††Significant for all pairwise comparisons except MCI vs non-AD (p = 1.00)

Table 2

Comparison of subjects with concordant T-status across all modalities and subjects with discordant T-status in at least one modality pair. Mean ± SD is shown for continuous variables

	Concordant T− (*n* = 99)	**Concordant T+ (*n* = 107)**	**Discordant T status (*n* = 145)**	***p* value***
Age	68.1 ± 8.3	68.4 ± 9.3	73.7 ± 8.5	$p < .001^{\dagger}$
Sex (M, %)	39 (39%)	39 (36%)	78 (54%)	$p = .01$
Education	15.6 ± 3.9	15.4 ± 3.3	15.5 ± 3.6	$p = .83$
MMSE	28.3 ± 2.5	23.2 ± 5.0	26.9 ± 4.6	$p < .001^{\dagger}$
Amyloid status (Aβ+, %)	14 (14%)	106 (99%)	76 (52%)	$p < .001$
CSF PTau181 (pg/mL)	16.1 ± 4.2	42.4 ± 16.6	23.2 ± 8.5	$p < .001$
FTP SUVR	1.14 ± 0.1	1.97 ± 0.5	1.28 ± 0.3	$p < .001$
Diagnosis (% Aβ+)	52 CN (15%)	9 CN (89%)	66 CN (48%)	$p < .001$
	23 MCI (17%)	38 MCI (100%)	45 MCI (42%)	
	2 AD_c (0%)	59 AD_c (100%)	23 AD_c (96%)	
	22 non–AD (9%)	1 non-AD (100%)	11 non-AD (27%)	

*p values shown for Kruskal-Wallis H test for continuous variables, and x^2 for nominal variables

†Bonferroni-corrected p values for pairwise comparisons are all < .001 except; T− vs discordant T for age ($p = 1.0$), and T– vs discordant T for MMSE ($p = .06$)

Eur J Nucl Med Mol Imaging. Author manuscript; available in PMC 2022 July 01.

Table 3

Sensitivity and specificity by modality. Multiple gold standard for evaluation of sensitivity and specificity were used; first, clinical gold standard (i.e., detection of Aβ + MCI and AD patients vs all other subjects), second, amyloid status alone (Aβ + vs Aβ−), and lastly, pathology in a small subsample (using moderate-to-high ADNC as gold standard). 95% CI values for sensitivity and specificity are shown in parentheses

	FTP visual assessment	FTP SUVR quantification	CSF PTau181
Gold standard: clinical (*n* = 351)			
Sensitivity	0.96 (0.91–0.98)	0.85 (0.78–0.91)	0.73 (0.64–0.80)
Specificity	0.60 (0.53–0.67)	0.91 (0.87–0.95)	0.72 (0.65–0.78)
Gold standard: Aβ status (*n* = 351)			
Sensitivity	0.89 (0.84–0.93)	0.68 (0.60–0.74)	0.66 (0.59–0.73)
Specificity	0.70 (0.62–0.77)	0.96 (0.92–0.99)	0.79 (0.72–0.85)
Gold standard: pathology (*n* = 11)			
Sensitivity	1.00 (0.54–1.00)	0.83 (0.36–1.00)	0.50 (0.12–0.88)
Specificity	1.00 (0.48–1.00)	0.80 (0.28–0.99)	0.80 (0.28–0.99)